

## Atmospheric N and P deposition in the Ganges Basin

The atmosphere–land–water connectivity of nutrients is not altogether accounted for in the Ganges Basin despite recent studies highlighting its importance<sup>1</sup>. Together with surface inputs, rivers receive N and P through atmospheric deposition (AD), directly on water surfaces, and through lateral transport. Globally, anthropogenic-input of reactive nitrogen (Nr) has increased from ~15 Tg in 1860 to 187 Tg by 2005 (ref. 1) and is predicted to be doubled by 2050 (ref. 2). A simple calculation from model estimates<sup>2,3</sup> shows that ~66% area of the Western Ghats, 42% of Indo-Burma and 9% of the Himalaya receive AD-Nr >15 kg ha<sup>-1</sup> yr<sup>-1</sup>, sufficient to affect terrestrial<sup>4</sup> and aquatic<sup>5</sup> ecosystems. Globally, annual P supply from atmospheric sources is ~3.7 Tg (ref. 6). Recent studies have shown AD-P in the northern Indian Ocean is comparable in magnitude to its riverine supply<sup>7,8</sup>. However, data on AD-P for terrestrial landscape of the region are limited. Here we show, from a watershed scale study, that atmospheric deposition in the Ganges Basin adds 107.47–406.54  $\mu\text{mol Nr m}^{-2} \text{d}^{-1}$  and 1.31–7.75  $\mu\text{mol P m}^{-2} \text{d}^{-1}$ , the values high enough to alter the ecology of the Ganga River and has significance for policy makers grappling to rejuvenate the river.

We collected samples of bulk atmospheric deposition/precipitation from 26 locations representing urban–rural sources of energy consumption, travel and food production along 2303 km transect from Dev Prayag (30°09'N, 78°30'E) to Ganga Sagar island (21°80'N 88°10'E). Climatic conditions vary from subtropical to tropical monsoonal with extended dry periods and westerly winds in western–central regions. Samples were collected seasonally between 2007 and 2014 (sites 8, 9, 14 and 15; Figure 1); 2012–2014 (sites 16–26), and in summer–monsoon 2012–2014 (sites 1–7 and 10–13) and analysed for  $\text{NH}_4^+$ ,  $\text{NO}_3^-$  and  $\text{PO}_4^{3-}$  spectrophotometrically. Significant effects of site and time series were evaluated using analysis of variance. Coefficient of variation (cv) was employed to measure data uncertainty and principal component ordination for site scaling.

AD- $\text{NO}_3^-$ -N in the watershed ranged from 50.73 to 142.24  $\mu\text{mol m}^{-2} \text{d}^{-1}$  (cv 23–28); AD- $\text{NH}_4^+$ -N from 56.72 to 264.30 (cv 18–26) and AD- $\text{PO}_4^{3-}$ -P from 1.31 to

7.75  $\mu\text{mol m}^{-2} \text{d}^{-1}$  (cv 28–34) (Table 1). Inputs were relatively higher in the middle sub-watershed followed by sites in the lower and upper sub-watersheds. AD-Nr and AD-P were log-normally distributed with fluxes being much larger in agriculturally intensified areas and downwind cities. At Dev Prayag, Varanasi and Kolkata urban sites, annual AD- $\text{NO}_3^-$  was 323.87, 494.46 and 434.41  $\mu\text{mol m}^{-2} \text{d}^{-1}$  respectively, with 6.0%, 8.6% and 6.5% annual increase; AD- $\text{NH}_4^+$  was 119.43, 218.00 and 204.25  $\mu\text{mol m}^{-2} \text{d}^{-1}$  respectively with 5.8%, 8.2% and 6.1% annual increase, and AD- $\text{PO}_4^{3-}$  was 11.03, 17.98 and 17.34  $\mu\text{mol m}^{-2} \text{d}^{-1}$  respectively, with 7.2%, 8.8% and 7.9% annual increase. In some urban sites, AD-Nr ( $\text{NH}_4^+ + \text{NO}_3^-$ ) exceeded 40 kg ha<sup>-1</sup> yr<sup>-1</sup> with ~2.62 kg ha<sup>-1</sup> or 8.8% annual increase. These values, although relatively lower than those observed in industrial and agriculturally intensified areas of China<sup>9</sup>, are along a similar trajectory to that previously experienced by the United States and Western Europe in the 1980s (ref. 10). Human activities such as food production, travel and energy consumption are accountable for rising AD inputs<sup>9</sup>. Occupying 26.2% of the total land area of India, the Ganges Basin with extensive

agricultural land (73.44% of total basin area) receives massive amount of agricultural fertilizers. Principal component ordination separating such sites from the remainder of the study transect clearly indicates agriculturally driven influences. About 55% of fertilizer N applied to croplands is redistributed to atmosphere as  $\text{NO}_x$  and  $\text{NH}_3$ , and 70–80% of this emitted N is deposited back to land surfaces<sup>11</sup>. Assuming a 50% loss through trans-boundary meteorological transport and other means, quantification from our data and the range of fertilizer applications (50–120 kg ha<sup>-1</sup>) in Ganges Basin indicates that agriculture alone, excluding livestock sources of emission, contributes >12.5 kg ha<sup>-1</sup> annually accounting ~40% of total AD-Nr in the watershed.

AD- $\text{NO}_3^-$  appeared a dominant vector although  $\text{NH}_4$ -N to  $\text{NO}_3$ -N ratios showed variable trends, being high (>1.6) in remote areas indicating increased contribution of agricultural sources<sup>9</sup>. In addition, the Ganges Basin suffers from intense dust storms of western origin<sup>12</sup> and massive accumulation of aerosols<sup>13</sup>. Thus, the synergy of atmospheric transformation, dominant westerly wind and forest edge effect could further enhance AD input even in least disturbed study locations, such as site 6. On the contrary,

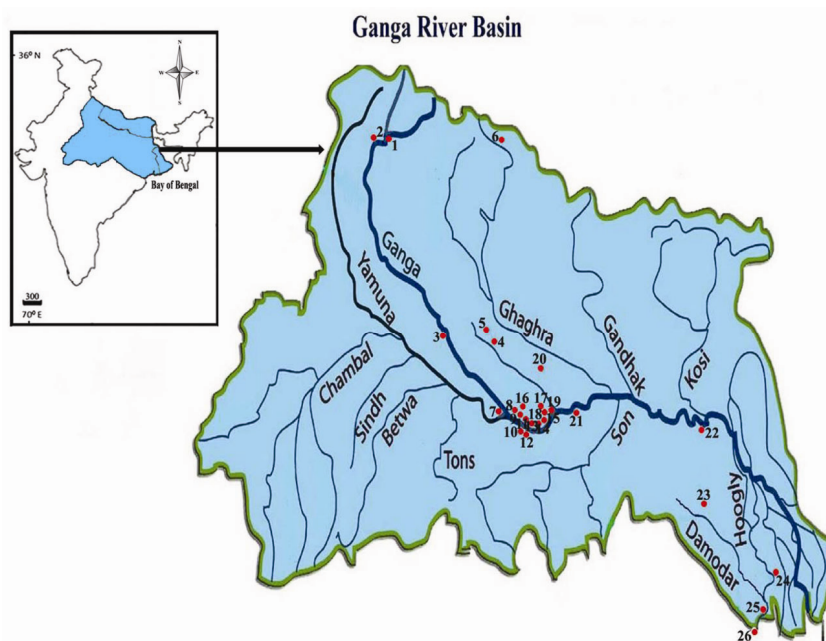


**Figure 1.** Ganges Basin showing the study locations. Description of study locations 1–26 is given in Table 1.

**Table 1.** Atmospheric deposition fluxes ( $\mu\text{mol m}^{-2} \text{d}^{-1}$ ) and descriptive statistics of nutrients in the Ganges Basin

Site	Location	<i>n</i> *	$\text{NO}_3\text{-N}$			$\text{NH}_4\text{-N}$			$\text{PO}_4^{3-}\text{-P}$		
			Mean	Range	CV	Mean	Range	CV	Mean	Range	CV
1	Devprayag	12	73.13	48.52–96.23	31	92.80	67.91–122.50	17	3.46	1.72–4.62	18
2	Hardwar	16	77.97	43.57–90.93	26	96.93	63.38–155.38	21	3.84	1.79–4.55	16
3	Kanpur	16	109.50	68.49–134.85	23	169.10	110.51–239.67	25	5.96	3.33–7.95	24
4	Lucknow	24	97.12	55.02–122.54	24	158.45	97.86–200.39	19	5.30	3.28–7.83	26
5	Sitapur	24	93.25	48.68–118.25	31	163.11	107.85–234.34	27	5.13	3.54–6.69	27
6	Katerniaghat	9	82.18	36.84–109.62	29	161.11	101.86–254.31	29	3.43	1.87–4.92	31
7	Allahabad	24	101.38	67.71–119.95	25	155.38	103.86–216.36	23	6.11	3.36–7.42	23
8	Adalpur	96	69.03	36.76–77.39	14	102.79	56.72–140.87	18	2.90	1.69–3.28	16
9	Sultankeshwar	92	75.76	43.61–90.35	18	107.18	69.50–181.08	22	3.08	1.72–3.33	21
10	Shahpur	24	97.51	63.84–120.72	21	166.43	87.21–237.80	24	3.43	1.92–3.74	27
11	Tadia	24	95.80	54.87–110.43	26	154.58	85.21–228.34	23	3.61	2.12–4.24	22
12	Ramnagar	24	109.11	62.68–125.79	32	163.24	96.93–251.65	26	3.61	2.02–4.49	26
13	BHU	24	76.81	51.58–88.22	27	121.83	69.90–201.05	29	3.11	1.92–3.71	22
14	Assighat	96	105.05	69.26–120.72	28	166.43	112.38–247.65	27	4.24	2.78–6.01	29
15	Rajghat	96	118.25	83.19–142.24	28	173.89	118.50–264.30	26	7.50	5.18–7.75	34
16	Lahartara	36	105.25	71.58–131.56	32	162.44	107.18–231.14	23	5.91	4.22–7.22	24
17	Shivpur	32	104.67	66.55–129.82	27	165.10	114.77–225.02	25	6.09	4.17–7.02	23
18	Sarnath	24	91.59	59.20–107.65	24	128.75	77.89–227.82	22	4.34	2.90–5.71	21
19	Markandeji	32	99.44	62.76–116.27	30	159.24	103.86–234.34	27	5.18	3.33–6.74	28
20	Azamgarh	36	81.91	50.73–96.73	23	156.32	92.54–215.43	22	4.09	3.28–5.00	23
21	Buxar	24	94.80	65.97–122.89	23	144.73	107.85–233.01	25	5.66	4.04–6.97	19
22	Bhagalpur	24	100.60	64.93–119.37	32	157.78	102.12–242.59	29	5.81	3.91–7.07	21
23	Durgapur	16	104.86	71.51–131.75	35	170.43	111.18–253.65	25	6.09	4.14–7.25	27
24	Kolkata	24	98.09	62.10–103.97	29	158.71	96.13–259.64	22	5.66	3.64–6.89	25
25	Diamond Harbour	16	89.0	57.65–102.73	36	129.95	78.56–222.36	27	4.19	2.65–5.33	27
26	Sagar island	9	79.59	79.59–94.80	35	109.18	70.57–187.74	26	2.45	1.31–3.89	28

\*Number of samples collected during the sampling period; CV, Coefficient of variation.

coal-based power plants, industrial activities and motor vehicles are major sources of  $\text{NO}_x$  in urban–industrial areas driving a more rapid increase in  $\text{NO}_x$  emission and consequently, relatively lower  $\text{NH}_4\text{-N}$  to  $\text{NO}_3\text{-N}$  ratios<sup>9</sup>. Significant negative relationship ( $R^2 = 0.67$ ;  $P < 0.001$ ) between AD- $\text{NO}_3$  and distance from the urban centres explains source variability<sup>14</sup>, although long-range transport and biogeochemical variability may mask such relationships<sup>15</sup>. AD- $\text{NO}_3$  recorded in this study is 1.5–2.5 fold higher than that measured about two decades ago in an urban location in the Upper Gangetic plains<sup>16</sup>, indicating a rising trend.

AD-P was 1.20–2.0 fold higher in Varanasi mostly due to enhanced biomass burning (~25,000 tonnes wood is burnt for cremation of ~36,000 dead bodies annually)<sup>17</sup>. Fertilizer application and biomass burning are major sources of continental atmospheric P (refs 7, 18). Earlier studies in Ecuador<sup>19</sup> and Varanasi<sup>20</sup> have also shown that increases in AD-P were relatively greater than those of AD-N causing a reduction in N : P

ratios, indicating relatively more P emission from biomass burning and other sources. Mineral dust is another important source of atmospheric P (ref. 6). Atmospheric P transport from Asia accounted for major fraction of soil P during four million years of ecosystem development in Hawaii<sup>21</sup>, with annual deposition rates  $>2.5 \text{ kg ha}^{-1}$ . AD-P flux in the Ganges Basin appears significantly higher compared to the model results<sup>22</sup>. An underestimate of AD-P by the models could arise due to inappropriate parameterization of contributions from local and regional sources and warrants the need for extensive original database and reassessment of model parameters in the light of potential emission sources<sup>6</sup>.

AD input fertilizes wider areas leading to a cascade of effects, including C- and N-fixation, soil stimulation, lateral transport of carbon and nutrients, rising DOC in surface waters and tightly coupled interactions with major biogeochemical cycles. Our study shows that the Ganges Basin receives ~3.32 Tg Nr ( $\text{NO}_3 + \text{NH}_4$ ) and ~173.20 Gg P ( $\text{PO}_4^{3-}$ ) annually. We argue that this additional supply would

contribute, potentially on similar scale, large fluxes of N and P to the Ganga River through watershed discharge<sup>23</sup>. Coupling stoichiometric mass balance of AD-inputs and gross primary productivity (GPP) of the Ganga River<sup>20</sup>, AD-N would result in fixation of 463.10–2667.90  $\mu\text{mol C m}^{-2} \text{d}^{-1}$ , while AD-P would be responsible for 137.56–813.71  $\mu\text{mol C m}^{-2} \text{d}^{-1}$  accounting 11.6–33.3% (for N) and 3.4–10.2% (for P) of GPP in the river. Since small but sustained P subsidies determine whether primary productivity is limited by P or N (ref. 24), a consistently rising AD-flux is expected to become an increasingly important determinant of the Ganges ecology. Since atmosphere–land–water connectivity is central to C budgeting, which has been largely a neglected issue in this region, we suggest that the Ganga River rejuvenation strategies should, in addition to sewage treatment and flow regulation, also address the significance of critical nutrients, especially N and P being added through atmospheric deposition. Refocusing research integrating these issues would help

policy makers grappling to rejuvenate the river.

- Galloway, J. N. *et al.*, *Science*, 2008, **320**, 889–892.
- Galloway, J. N. *et al.*, *Biogeochemistry*, 2004, **70**, 153–226.
- Phoenix, G. K. *et al.*, *Global Change Biol.*, 2006, **12**, 470–476.
- Clark, C. M. and Tilman, D., *Nature*, 2008, **451**, 712–715.
- Elser, J. J. *et al.*, *Science*, 2009, **326**, 835–837.
- Tipping, E. *et al.*, *Environ Sci: Process. Impacts*, 2014, **16**, 1608–1617.
- Srinivas, B. and Sarin, M. M., *Sci. Total Environ.*, 2013, **456–457**, 104–114.
- Srinivas, B. and Sarin, M. M., *Curr. Sci.*, 2015, **108**, 1–6.
- Liu, X. *et al.*, *Nature*, 2013, **494**, 459–462.
- Holland, E. A., Braswell, B. H., Sulzman, J. and Lamarque, J. F., *Ecol. Appl.*, 2005, **15**, 38–57.
- Galloway, J. N., Schlesinger, W. H., Levy, I. H., Michaels, A. and Schnoor, J. L., *Global Biogeochem. Cycles*, 1995, **9**, 235–252.
- Kumar, S. *et al.*, *Aeolian Res.*, 2015, **17**, 15–31.
- Dey, S. and Tripathi, S. N., *J. Geophys. Res.*, 2007, **112**, D03203.
- Lovett, G. M., Traynor, M. M., Pouyat, R. V., Carreiro, M. M., Zhu, W. and Bayter, J. W., *Environ. Sci. Technol.*, 2000, **34**, 4294–4300.
- Lohse, K. A., Hope, D., Sponseller, R., Allen, J. O. and Grimm, N. B., *Sci. Total Environ.*, 2008, **402**, 95–105.
- Saxena, A. *et al.*, *Atmos. Environ.*, 1997, **31**, 2361–2366.
- Pandey, J., Pandey, U. and Singh, A. V., *Biogeochemistry*, 2014, **119**, 179–198.
- Venkataraman, C. *et al.*, *Global Biogeochem. Cycles*, 2006, **20**, GB2013.
- Boy, J. and Wilcke, W., *Global Biogeochem. Cycles*, 2008, **22**, GB 1027, 1–11.
- Pandey, J., Pandey, U. and Singh, A. V., *Curr. Sci.*, 2014, **107**, 956–958.
- Chadwick, O. A., Derry, L. A., Vitousek, P. M., Huebert, B. J. and Hedin, L. O., *Nature*, 1999, **397**, 491–497.
- Mahowald, N. *et al.*, *Global Biogeochem. Cycles*, 2008, **22**, GB4026.
- Beman, J. M. *et al.*, *Nature*, 2005, **434**, 211–214.
- Camarero, L. and Catalan, J., *Nature Commun.*, 2012, **3**, 1118.

ACKNOWLEDGEMENTS. We thank the Head, Department of Botany, Banaras Hindu University, Varanasi for providing the facilities. Part of this study was funded by UGC, New Delhi (Project No. 32-383/2006/SR). We

also thank the National Academy of Sciences (India), Allahabad for Ganga Research Fellowship to A.V.S. and CSIR, New Delhi for Junior Research Fellowship to S.T.

Received 30 July 2015; revised accepted 27 October 2015

J. PANDEY<sup>1,\*</sup>  
U. PANDEY<sup>2</sup>  
A. V. SINGH<sup>1</sup>  
S. TRIPATHI<sup>1</sup>  
V. MISHRA<sup>3</sup>

<sup>1</sup>*Environmental Science Division, Centre of Advanced Study in Botany, Banaras Hindu University, Varanasi 221 005, India*

<sup>2</sup>*Department of Botany, Faculty of Science and Technology, Mahatma Gandhi Kashividyapith, Varanasi 221 002, India*

<sup>3</sup>*Department of Chemistry, Maulana Azad Institute of Humanity, Science and Technology, Sitapur 261 203, India*

\*For correspondence.  
e-mail: jiten\_pandey@rediffmail.com

## Artificial pollination and fruit set in double coconut growing in India

The double-coconut palm [*Lodoicea maldivica* (J.F. Gmel.) Pers. (family: Arecaceae)] of Seychelles is one of the most interesting plant species of the world<sup>1</sup>. The seed of this palm resembles two coconuts fused together; hence the name ‘double coconut’<sup>2</sup> (Figure 1a). The pollination mechanism in double coconut remains unclear, with a prevalent popular belief that the species is wind-pollinated<sup>3</sup>. In staminate (male) flowers, nectaries are situated on the margins of the bract. Both male and female flowers emit a strong, musty, sweet smell. Only a few pistillate flowers are receptive on any palm at a given time<sup>3</sup>. The recent work of Blackmore *et al.*<sup>4</sup> has thrown light on its morphology and pollination biology.

A single plant of double coconut was raised in Acharya Jagadish Chandra Bose Indian Botanic Garden (AJCIBG), Botanical Survey of India (BSI), Howrah (the erstwhile Indian Botanic Garden or Company’s Bagan at Howrah) using seeds obtained from Seychelles in 1894

and planted in the central part of the Large Palm House. It is the only palm of double coconut that now exists in India (Figure 1b); it has bloomed for the first time in the end of October 1988 and bore female flowers<sup>5</sup>. The inflorescence, approximately 1 m in length, persisted for about 2 years. However, there was no fruit set because of the absence of male plants. Now, the height of the plant is about 10 m and it produces one leaf per year. Presently, its crown bears 12 fully expanded green leaves (bottom three leaves are much older), one half expanded and one spear-like emerging leaf. An emerging leaf takes approximately 1.5 years for full expansion<sup>6</sup> (Figure 1c).

In the year 2006, emergence of only two inflorescences was noticed on this tree (previous records were not kept). Thereafter, 2–4 inflorescences appeared every year. The length of inflorescences was  $92.76 \pm 6.81$  cm (mean  $\pm$  SD) and the number of female flowers in each cluster varied from 3 to 9. The total

number of female flowers in each inflorescence was proportional to the length of the inflorescence. The average size (mean  $\pm$  SD) of a female flower at the receptive stage was  $10.83 \pm 1.07$  cm in length and  $30.86 \pm 0.99$  cm across (measurement made along with perianth on 15 flowers from 7 inflorescences). The female flowers are borne singly within a pair of broad bracts and comprise of six perianth lobes, sheathing a conical ovary with sessile stigma. In the Garden, the emergence of female inflorescence is noted from the middle of March to middle of September. It emerges from inside the leaf sheath with pointed tips and slowly grows in a zigzag manner bearing several empty, incompletely sheathing bracts and the subsequent ones with complete sheathing. It takes more than a month for the full growth of female inflorescence and another 10–15 days for the female flower to attain the receptive stage (Figure 1d).